

IN-SITU MEASUREMENT OF THE ELECTRICAL CONDUCTIVITY OF ALUMINUM OXIDE IN HFIR - S.J. Zinkle, D.P. White, L.L. Snead, W.S. Eatherly, A.L. Qualls, D.W. Heatherly, R.G. Sitterson, R.L. Wallace, D.G. Raby and M.T. Hurst (Oak Ridge National Laboratory), E.H. Farnum and K. Scarborough (Los Alamos National Laboratory), T. Shikama and M. Narui (Tohoku University), and K. Shiiyama (Kyushu University)

OBJECTIVE

The objective of this work is to determine the existence or absence of bulk radiation induced electrical degradation (RIED) in neutron-irradiated Al_2O_3 .

SUMMARY

A collaborative DOE/Monbuscho irradiation experiment has been completed which measured the in-situ electrical resistivity of 12 different grades of aluminum oxide during HFIR neutron irradiation at 450°C. No evidence for bulk RIED was observed following irradiation to a maximum dose of 3 dpa with an applied dc electric field of 200 V/mm.

PROGRESS AND STATUS

Introduction

Ceramic insulators are required for the heating, control and diagnostic measurement of magnetically confined plasmas [1]. A potentially serious degradation of the electrical resistance of ceramic insulators, known as radiation induced electrical degradation (RIED), has raised concern about the suitability of ceramic insulators in intense radiation fields [1-5]. Since the original reported observation of RIED by Hodgson in 1989 [4], numerous studies have been performed with conflicting results (see ref. 3 for a recent summary). Previous studies indicate that RIED is most pronounced at temperatures between 300 and 600°C and at applied voltages >100 V/mm, with an apparent maximum degradation rate occurring near 450°C. Therefore, the present HFIR experiment was chosen to be performed at 450°C with an applied potential of 200 V/mm. The experiments were performed in the Temperature-Regulated In-Situ Test (TRIST) facility located in a Removable Beryllium position of the High Flux Isotope Reactor (HFIR) at Oak Ridge National Laboratory (ORNL). A total of 15 specimens were irradiated in the in-situ electrical conductivity capsule. The specimen matrix included 12 different grades of polycrystal and single crystal alumina (Table 1) in order to confirm published studies which suggested that the threshold dose for initiation of RIED depends on specimen purity [5,6].

Experimental Procedure

The Al_2O_3 specimens were machined into disks that were 8.5 mm diameter by 0.75 mm thick. The specimens were vacuum brazed at 870°C to alumina pedestals using a Ticusil braze foil. This braze material covered the entire bottom surface of the sample and the top of a nickel pin which served as the rear electrode. The alumina pedestal was simultaneously vacuum brazed to a vanadium heat sink using Ticusil braze foil. InCuSil braze pads were applied to the center and guard electrode regions on the top surface of the alumina specimens. Nickel wires were subsequently laser welded to the braze pads to provide a secure electrical connection. Metallic electrodes were then sputtered onto the specimens in a guard ring configuration with a 4 mm central electrode diameter and a 1.0 mm gap between the central electrode and the guard ring. The electrodes were deposited as a thin layer (<0.1 μm) of titanium followed by ~1 μm Pt layer using a two-gun vacuum deposition system. Ohmic behavior of the Ti + Pt electrodes (in the absence of irradiation) was verified for a Wesgo AL995 and sapphire specimen. All of the subcapsules were sealed to minimize the amount of surface contamination buildup during irradiation.

Table 1: Specimen list for the HFIR TRIST-ER1 in-situ electrical conductivity capsule.

HFIR position	Material	Appl. Voltage	Vendor and grade
1	Al ₂ O ₃ , single crystal	150 V	Crystal Systems (Hemex UV grade) a-axis
2	Al ₂ O ₃ , single crystal	150 V	Crystal Systems (Hemex UV grade) c-axis
3	Al ₂ O ₃ , single crystal	150 V	Crystal Systems (Hemex regular) c-axis
4	Al ₂ O ₃ , single crystal	150 V	Crystal Systems (Hemex regular) a-axis
5	Al ₂ O ₃ , polycrystalline	150 V	Vitox (99.9% purity, Morgan Matroc, Anderman Div.)
6	Al ₂ O ₃ , polycrystalline	150 V	Kyocera A-480 (99.9% purity)
7	Al ₂ O ₃ , polycrystalline	150 V	Wesgo AL300 (97.0% purity)
8	Al ₂ O ₃ , polycrystalline	150 V	Kyocera A-479 (99.0% purity)
9	Al ₂ O ₃ , polycrystalline	150 V	Coors AD998 (99.8% purity)
10	Al ₂ O ₃ , polycrystalline	150 V	Wesgo AL995 (99.5% purity)
11	Al ₂ O ₃ , polycrystalline	0 V	Wesgo AL995 (99.5% purity)
12	Al ₂ O ₃ , single crystal	0 V	Crystal Systems (Hemex regular) c-axis
13	Al ₂ O ₃ +Cr, single crystal	150 V	Union Carbide (UV grade), 60° from c axis
14	Al ₂ O ₃ , single crystal	150 V	Kyocera SA100 (1 $\bar{1}$ 02 orientation)
15	Al ₂ O ₃ , single crystal	0 V	Kyocera SA100 (1 $\bar{1}$ 02 orientation)

A total of 60 stainless steel sheathed, mineral insulated (MI) cables were used to instrument the samples contained in the subcapsules. A 1.1 mm OD triaxial MI cable with a copper center wire and a braided copper sheath was used as the low-side data lead from each subcapsule. A 1.6 mm OD coaxial MI cable with a copper center conductor was used as the power lead. The leads for the coax and triax cables were torch-brazed to the appropriate Ni wires from each subcapsule. The line resistances of the MI coaxial and triaxial cables were all $\sim 1 \Omega$. The specimen temperatures were continuously monitored by two chromel/alumel (type K) thermocouples embedded in each subcapsule. Further details about the capsule design and assembly are given elsewhere [7].

The capsule was cooled with 49°C reactor coolant water flowing downward at a flow rate of 0.9 l/s, with a water temperature rise of 5°C over the length of the capsule. The sample temperatures were controlled by adjusting the composition of a flowing mixture of helium and neon in the control gas gap between the subcapsules and the holder sleeve [7,8]. The gas gap on the outside of each vanadium subcapsule body was sized, based on a thermal analysis and the known HFIR nuclear heating axial profile, to maintain an irradiation temperature of $\sim 450^\circ\text{C}$ during irradiation. The output of the 30 thermocouples was fed into a PC-based μDCS Plus control system. Operating temperatures, pressures, and flow rates were monitored continuously and trended at a rate of approximately once per 5 to 10 seconds. The measured irradiation temperatures for the 15 subcapsules ranged from ~ 440 to 500°C , depending on the subcapsule position. Details of the irradiation temperature history are described elsewhere [8].

The in-situ electrical measurements were performed in full accordance with the guidelines outlined in ASTM Standard Test Method for DC Resistance or Conductance of Insulating Materials (ASTM D257-91), and also followed the IEA guidelines established at a ceramics fusion energy workshop in Stresa, Italy [9]. In particular, the measurements utilized a guard ring configuration with secure, low resistance electrical connections and the dimensions of the electrodes met ASTM recommendations. Data acquisition and control was performed using a National Instruments Labview III program running on a Macintosh computer. A Keithley 7002 matrix switch system (containing Keithley 7169A switch cards on the high side and 7058 switch cards on the low side) was used to switch the specimen leads to the appropriate electrical instruments. A dc potential of 150 V was continuously supplied to the brazed base surface of 12 of the specimens (except for brief periods when electrical measurements were taken) by two HP 6035A power supplies, producing an electric field of 200 V/mm in the specimens.

Several different types of electrical measurements were performed on the specimens in order to differentiate between bulk conductivities and surface conductances. First, the specimen current through the guard and center electrode leads with an applied potential of 100 V was periodically measured in order to monitor the qualitative electrical conductivity of the specimens. A Keithley 237 Source Measure Unit was used to supply the specimen voltage and measured the corresponding current through the coax cable, and two Keithley 6517 high-resistance electrometers were used to measure the guard and center electrode currents for each specimen. A Keithley 617 electrometer was used to independently measure the potential supplied by the 237 power supply. These measurements were performed with a frequency of about twice per hour during the first five days of the irradiation, and about twice per day thereafter. In addition, measurements were taken more frequently (about 20 times per hour) during reactor startup and shutdown. Second, the ohmic nature of these electrical measurements was determined with the same set of electrical equipment over a typical potential range of +100 V to -100V with 20 V increments. These measurements were typically performed about once per day (more frequently during reactor startup and shutdown). A limited set of ohmic check measurements were also performed from +10 V to -10 V and from +150 V to -150 V on selected specimens in order to further study the electrical behavior. Third, a series of four types of diagnostic measurements were performed approximately twice per month which allowed the surface resistance and cable insulation conductivities to be measured. The first diagnostic test measured the leakage current from the center lead of each coax cable at voltages from +100 V to -100 V while the triax cable was floating. The other three diagnostic tests applied voltages from +2 V to -2 V in 0.5 V increments to the center and/or guard sheath of each triax cable. This allowed the center-guard and guard-ground resistances to be measured for each subcapsule/triax cable pair, and allowed the possible presence of gaseous conduction current paths to be detected. Finally, the ac impedance was measured over a frequency of 100 Hz to 10 MHz using an HP4194A Impedance/ Gain-Phase Analyzer. Further details regarding the electrical equipment, cabling, and Labview program capabilities are described elsewhere [10-13].

For each electrical measurement, a settling time of 20 to 30 seconds was typically used from the time the specimen was switched to the power supply until the electrical currents were measured in order to eliminate signal noise associated with the cable and specimen capacitance. Due to the long cable length (~20 m), the specimen capacitance was negligible (3 orders of magnitude smaller) compared to the cable capacitance. Similarly, the circuit resistance was mainly determined by the coax cable resistance, since the specimen and cable resistances were in parallel and the specimen resistance was typically 3 orders of magnitude larger than the cable resistance during irradiation. Using a calculated cable capacitance of ~10 pF and a typical cable resistance of 100 k Ω during irradiation, the calculated circuit RC time constant is ~1 ms, which is negligible compared to the settling times used for the data collection. During the reactor startup and shutdown, a settling time of 5 to 10 seconds was typically used in order to obtain data more rapidly. Experimental tests at applied potentials between +100 V and -100 V on several specimens during full-power HFIR irradiation demonstrated that the measured electrical currents were similar for settling times between 5 seconds and 180 seconds.

During the first five days of the irradiation, all of the biased specimens which were not undergoing an electrical measurement were left connected to the 150 V dc bias from the HP power supplies. This was performed in order to minimize the amount of time that the "biased" samples were exposed to irradiation with the electric field turned off. However, this arrangement had a disadvantage of producing current spikes in the coax cables during the switching operations, particularly when specimens were switched from an ohmic check measurement at -100 V back into the bias circuit at +150 V. Large transient electrical currents were observed on the power supply current meter during these switching operations, some of which blew the 0.5 A fuses installed on the individual coax cable leads. Larger fuses (1 A) were installed in an attempt to eliminate blown fuses. However, several of the electrical cables failed (electrical short) over a period of several days due to the high transient currents. The Labview program was modified after five days of irradiation to shut off the 150 V bias during electrical measurements, and to slowly ramp the power supply from 0 to 150 V when the bias was reapplied following completion of a set of electrical measurements. The frequency of electrical measurements was reduced to ~ two per day when this change was implemented in order to minimize the amount of time that specimens were irradiated without the 150 V bias. The 150 V potential was applied to the biased specimens ~98% of the total irradiation time.

The irradiation was accomplished over a time period of about three and one half months, and involved three irradiation cycles (each ~26 days) of the HFIR reactor operating at 85 MW. The electrical conductivity of the specimens was measured before, during and following each of the three HFIR irradiation cycles. Due to the relatively low levels of nuclear heating when the reactor was not at full power, the specimen temperatures could not be maintained at 450°C when the reactor was off or at 10% power. The capsule was initially installed in the HFIR pool on Feb. 23, 1996 during the refueling outage between reactor cycles 343 and 344, and a series of preirradiation electrical measurements were performed for two weeks prior to the start of the irradiation. The capsule was installed in the HFIR core on March 4, 1996, and reactor startup occurred on March 8, 1996. The irradiation capsule reached its target centerline fluence of $\sim 3 \times 10^{25}$ n/m² (E>0.1 MeV) on June 20, 1996, which corresponds to a damage level of ~ 3 dpa in alumina. The irradiation temperature was maintained at 440 to 500°C for all 15 specimens during the irradiation. The full-power reactor ionizing dose rate [8] was 10 to 16 kGy/s and the average displacement damage rate was ~2.4 to 4.3×10^{-7} dpa/s, with the lowest dose rates obtained for subcapsules 1 and 15 and the highest dose rate for subcapsule 8 (Table 2). The ionizing dose rate in the core with the reactor turned off (spent fuel removed) was dominated by the EuO₂ control plates, and the dose rate at the capsule location was estimated by HFIR staff to be ~10 Gy/s. Further analysis is underway to verify the quantitative accuracy of this reactor-off ionizing dose rate. 12 of the 15 specimens were irradiated with a dc bias of 150 V (electric field of 200 V/mm), with the remaining three specimens irradiated without dc bias (Table 1). The experimental matrix included 7 high purity single crystal alumina (sapphire) specimens (2 of which were irradiated without dc bias), including UV grade and normal grade sapphire with 3 different crystallographic orientations. A Cr-doped sapphire specimens was also irradiated under dc bias, and the remaining 7 specimens were different grades of polycrystalline alumina obtained from 4 different vendors (Wesgo AL300, Wesgo AL995--with and without dc bias, Coors AD998, Kyocera A-479, Kyocera A-480, Vitox).

Results and Discussion

The specimens exhibited a typical resistivity $> 2 \times 10^{10}$ Ω-m (the maximum resistivity measurable with our system due to the ~1 TΩ resistance in the scanner cards) at 40°C prior to insertion in the reactor. The measured in-core resistivities of the 15 specimens are summarized in Table 2. The measured RIC was independent of crystallographic orientation, but was strongly dependent on specimen purity at low ionizing dose rates. The preirradiation in-reactor resistivities at a temperature of ~50°C (with ~10 Gy/s ionizing dose rate) ranged from ~0.3 to 10 GΩ-m for the different specimens. The lowest resistivities were obtained for the high-purity sapphire specimens, and the highest resistivities were observed for the polycrystalline specimens. The resistivities were obtained from the slope of the current vs. voltage (ohmic check) plots. The high-purity sapphire specimens generally exhibited approximately ohmic behavior at 10 Gy/s, whereas the polycrystalline specimens and the Cr-doped sapphire specimen exhibited moderate nonohmic behavior.

Figure 1 shows examples of the ohmic check data for four different specimens (samples 1,3,9 and 10) obtained from about 20 series of measurements performed over a period of 4 days prior to reactor startup. It can be seen that the ohmic check data for a given sample were generally very reproducible. The typical standard error in resistivity determined from the slope of an ohmic check curve was less than ±50%. Significant nonohmic behavior was observed in all 15 of the specimens in two nonsequential series of measurements, as demonstrated by the dashed curves in Fig. 1. The main controllable experimental parameters such as RC settling time (20 s) were held constant during these measurements, and the cause of the nonohmic behavior is uncertain. The nonohmic behavior occurred mainly in the positive quadrant of the current vs. voltage plot and consisted of a positive offset current of a few nA. All of the resistivities quoted in this report were obtained from the slope in the negative quadrant of the ohmic check curves. Further data analysis is planned to find a possible cause of this nonohmic behavior.

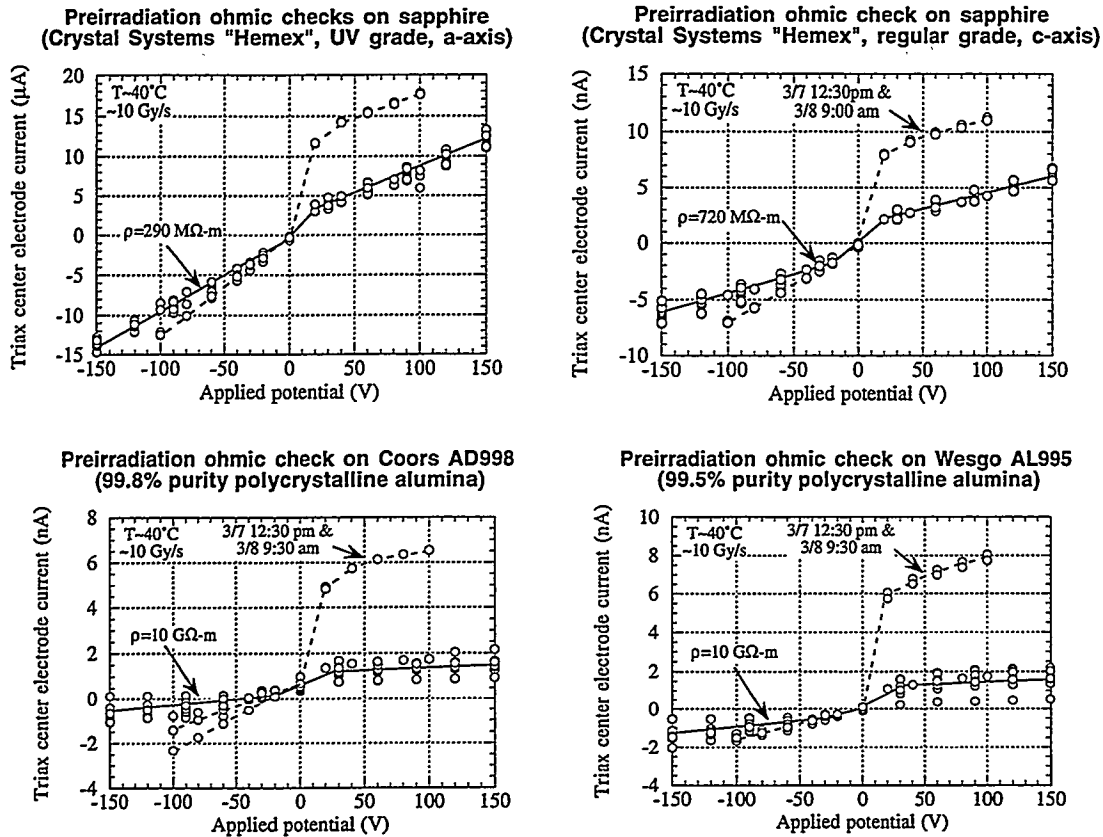


Fig. 1. Comparison of the preirradiation electrical behavior of four different grades of alumina (samples 1,3,9 and 10). The dashed curves represent atypical behavior that was observed on two separate (nonsequential) occasions during the last two days prior to reactor startup.

Table 2. Summary of measured in-core resistivities ($M\Omega\cdot m$) at the start of the irradiation (from the negative quadrant of the ohmic check plots). The data marked with an asterisk denote values that are a lower limit to the bulk resistivity due to low ($<100\text{ k}\Omega$) surface leakage resistances.

HFIR position	Material	Preirradiation (10 Gy/s, 50°C)	10% power, 0 dpa (1-1.6 kGy/s, 170°C)	full power, 0 dpa (10-16 kGy/s, 440-500°C)
1	UV sapphire, a-axis	300	28	7.7
2	UV sapphire, c-axis	300	16	3.0
3	regular sapphire, c-axis	700	20	5.6
4	regular sapphire, a-axis	700	12	3.0
5	Vitox	(>20)*	(>2.5)*	(>2)*
6	Kyocera A-480	10000	11	1.0
7	Wesgo AL300	7000	6	1.7
8	Kyocera A-479	10000	15	3.9
9	Coors AD998	10000	26	erratic
10	Wesgo AL995	10000	19	(>1.5)*
11	Wesgo AL995	10000	22	5.2
12	regular sapphire, c-axis	500	16	5.0
13	Cr-doped sapphire	5000	15	5.5
14	SA100 sapphire (1 $\bar{1}$ 02)	400	14	5.4
15	SA100 sapphire (1 $\bar{1}$ 02)	(>10)*	(>0.8)*	(>0.3)*

Figure 2 shows the electric currents measured at 100 V in two of the specimens during the initial stages of the first irradiation cycle. A nonconventional startup was used for this irradiation cycle (#344) in order to perform reactor operating training and to allow a full set of in-situ conductivity data to be obtained at an intermediate power level. For the first irradiation cycle, the reactor was brought to 10% power within 10 minutes and held at this power level for ~1.5 h. The reactor was then scrammed, and a conventional ascension to full power operation (~1 h from 0 to 100% power) was then followed. The specimen temperatures during the 10% power operation for this cycle were ~180°C, achieved by flowing Ar gas in the gas gap region outside of the subcapsules. The gas mixture was changed to He and Ne prior to ascension to full power.

The radiation induced conductivity (RIC) behavior was tested at 10% and full reactor power (~1-1.6 and 10-16 kGy/s, respectively), and was found to be sublinear for all of the specimens (Table 2). The material dependence of the RIC was small at 10% and full reactor power, in contrast to the strong material dependence observed at 10 Gy/s. It is interesting to note that the polycrystalline specimens generally had slightly lower resistivities than high-purity sapphire at 10% and full reactor power, which is opposite to the RIC behavior observed at 10 Gy/s. This change in material dependence of the RIC behavior may be partially due to temperature differences at the three dose rates. Further work is needed to determine role of irradiation temperature and dose rate on the RIC of these different grades of alumina. The typical resistivity at full reactor power (~15 kGy/s) was 3 to 5 MΩ-m for all of the specimens, which agrees well with previous RIC studies on alumina [2].

Approximately half of the high voltage coaxial cables failed (electrical short) during the course of the 3-month irradiation. The first five cable failures (in sequential order, subcapsules 6,10,14,5 and 1) occurred during the first five days of full power irradiation, where specimens were switched between the 150 V circuit and the electrical measurement circuit with the 150 V power supply turned on. Three additional cables (#12,7,8) failed after the Labview program was modified to turn off the power supply during electrical measurement and switching operations. One of these cable failures occurred after 16 days of irradiation in a "control" subcapsule (#12) which was not exposed to 150 V bias during the irradiation. The failure in two of the coax cables (#7,10) occurred near the end of an ohmic check measurement as the voltage was ramped from -80 V to -100 V. Figure 3 shows an example of the electrical current measured in the Wesgo AL300 specimen for the first two irradiation cycles. The specimen current at reactor full power decreased by about a factor of two as displacement damage was accumulated during the first irradiation cycle, and the measured conductivity during the subsequent HFIR shutdown at the end of the first cycle was comparable to the preirradiation conductivity. The coaxial cable for this specimen shorted approximately two days after the reactor was restarted for the second irradiation cycle. The failure occurred as an ohmic check measurement was being performed at -100 V. The data obtained at +100 V to -80 V immediately prior to the cable failure did not indicate any unusual behavior.

The cause of the coax cable failures is mostly likely due to dielectric breakdown in the glass seals used for the coaxial cable terminations; the maximum electric field in the glass seal at an applied potential of 150 V was ~1 MV/m, and the calculated operating temperature of the glass seals in the HFIR capsule was ~200°C. This temperature is close to the softening temperature of the Ferro 7556 lead borosilicate glass used to seal the HFIR MI cables (330°C). The typical dielectric breakdown strength (DBS) of glass is 10-100 MV/m at 20°C, and the DBS of glass decreases rapidly with increasing temperature above 20°C [14]. The DBS of the Ferro 7556 glass used in the HFIR irradiations will be experimentally measured in the near future. Simple diagnostic tests performed on the specimens with shorted coaxial cables demonstrated that the specimen bulk resistance was comparable to that of all of the other alumina specimens; therefore, the cable failure was not associated with RIED in the alumina specimens. These tests included measurement of the resistance between the coax cable and triax lead, and measurement of the surface resistances. A higher temperature grade of glass (EG3606 Zn borosilicate) that was successfully used in a previous RIED experiment at the HFBR reactor [13] was not utilized for the HFIR cables due to problems with impurity pickup that could not be resolved within the short amount of time available prior to the deadline for inserting the capsule into HFIR.

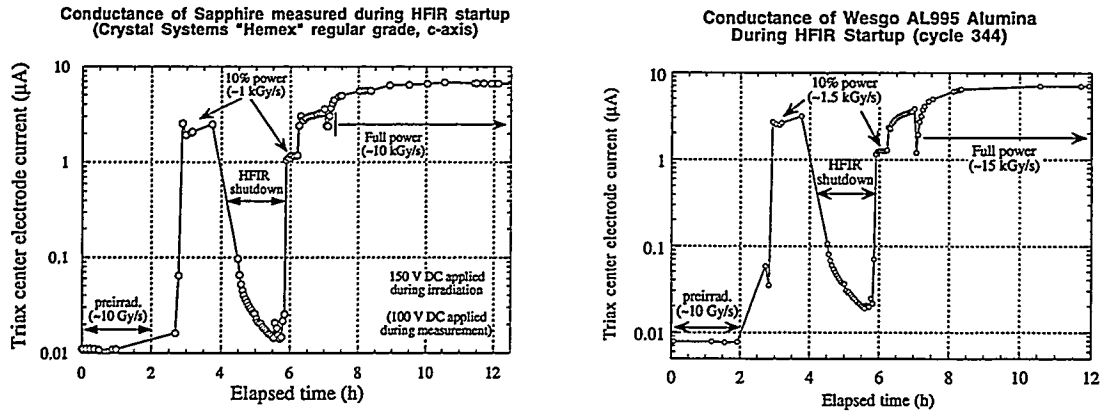


Fig. 2. Electrical currents measured in samples 3 and 10 during the first 12 hours of the irradiation.

Conductance of Wesgo AL300 During 1st and 2nd Cycles of HFIR Irradiation (cycles 344&345)

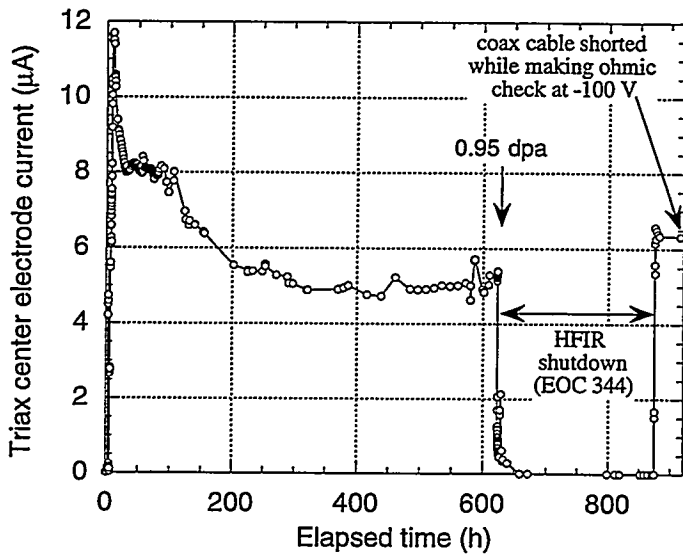


Fig. 3. Measured current at 100 V in Wesgo AL300 during the first two cycles of irradiation.

**Conductance of Sapphire Measured During HFIR Irradiation
(Crystal Systems "Hemex" UV grade, c-axis)**

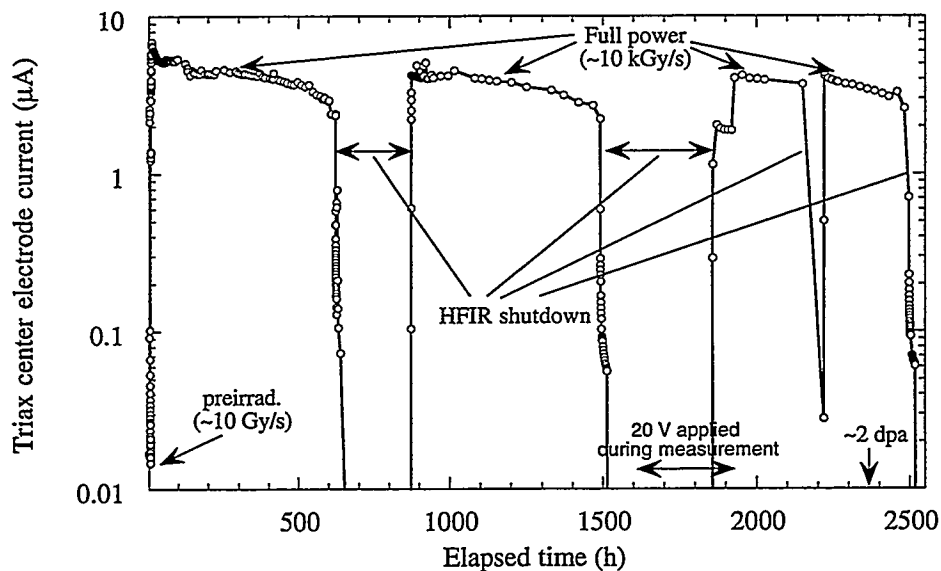


Fig. 4. Measured current at 100 V in UV grade sapphire (sample 2) during the three cycles of HFIR irradiation. The measurement voltage was 20 V for a brief period during the 3rd cycle, as indicated.

**Conductance of Sapphire Measured During HFIR Irradiation
(Crystal Systems "Hemex" regular grade, c-axis)**

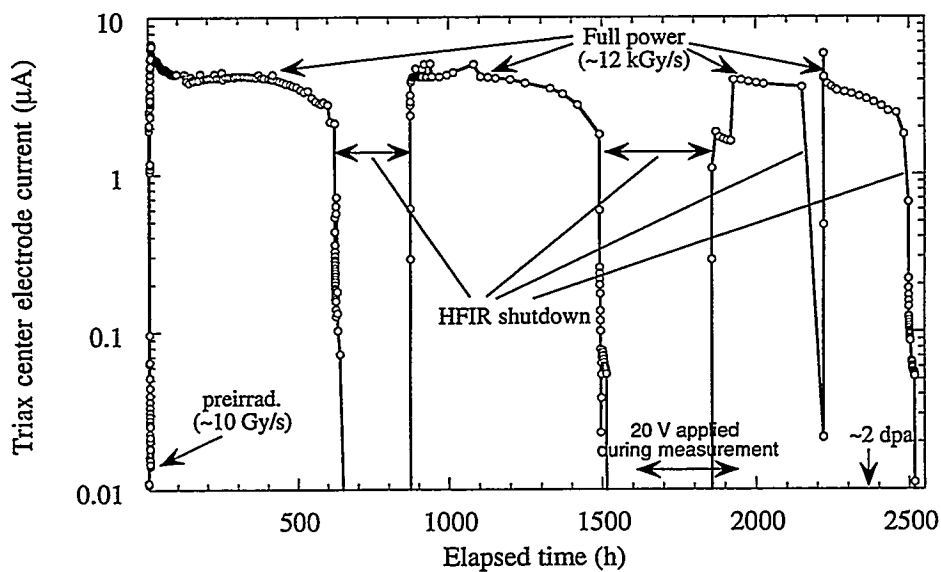


Fig. 5. Measured current at 100 V in regular grade sapphire (sample 3) during the three cycles of HFIR irradiation. The measurement voltage was 20 V for a brief period during the 3rd cycle.

No evidence for radiation induced electrical degradation (RIED) above the RIC level was observed during irradiation to 3 dpa at 450 to 500°C with a continuously applied dc electric field of 200 V/mm. It is particularly noteworthy that RIED was not observed in the sapphire specimens, which were found to have an incubation dose of <0.001 dpa for catastrophic RIED in electron irradiation studies [4,6]. Figures 4 and 5 show the electrical currents measured at 100 V in two sapphire specimens over the 3 HFIR irradiation cycles. The measured current decreased over the course of each irradiation cycle, due in part to changes in the ionizing radiation dose rate as the control rods were repositioned. Except for an initial ~50% decrease in current during the first 2 days of irradiation, the shape of the curves was similar for the 3 irradiation cycles. Two comments should be made regarding the third irradiation cycle. First, as evident from Figs. 4 and 5, a reactor scram occurred during the third irradiation cycle, and the reactor was restarted two days later. Second, the measurement voltage was inadvertently left at 20 V following some diagnostic tests performed prior to the third irradiation cycle, and was not changed back to 100 V until several days after the restart of the reactor. This produced a lower measured current for these data points. The bias voltage was maintained at 150 V on these specimens during this time period (except for brief interruptions to perform the electrical measurements).

The measured resistivity increased rapidly following reactor shutdown for each of the 3 irradiation cycles, and was typically ~5 to 10 GΩ-m at ~20°C in the irradiated sapphire specimens after removal from the HFIR core. These resistivities are slightly lower than that measured in pre-irradiation tests outside of the reactor (typically >20 GΩ-m), which is attributed to slight increases in surface leakage currents in the irradiation capsule. Most of the increased surface leakage occurred during the first irradiation cycle.

Figure 6 compares ohmic check measurements at ~0 and ~1 dpa in sapphire (sample 2) at two ionizing dose rates. The ohmic check data were obtained at the start of the first and second reactor cycles. A pronounced increase in resistivity (compared to the preirradiation value) was observed for all specimens at 10 Gy/s following irradiation to ~1 dpa. On the other hand, the resistivity increase between 0 and ~1 dpa was relatively small at 10% and full reactor power levels. This improvement in the electrical resistivity (which is opposite to the reported RIED effect) may be attributable to increased electron-hole trapping at radiation-produced defects, and is in agreement with previous studies performed on alumina where an electric field was not applied during the irradiation [1,2]. The resistivities measured at all three ionizing dose rates (10 Gy/s, ~1 kGy/s and ~10 kGy/s) showed no evidence of bulk RIED for doses up to 3 dpa. These results indicate that bulk RIED should not be a problem for good-quality alumina insulators in ITER and other fusion energy devices for doses up to at least several dpa. Additional postirradiation measurements at the irradiation temperature are planned to determine if any slight underlying amount of RIED has occurred.

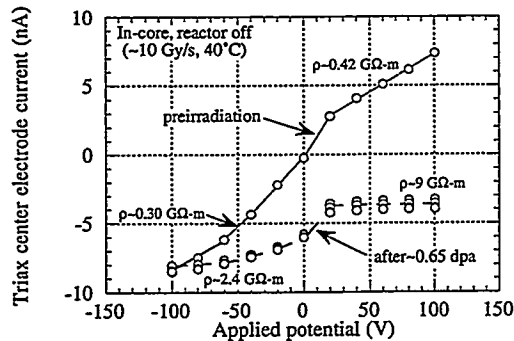
FUTURE WORK

Dielectric breakdown strength measurements will be performed in the next reporting period on the glass seals of several control MI coax cables from the HFIR experiment. The TRIST-ER1 capsule will be stored in the HFIR pool until about November 1996, and will then be taken to a hot cell for disassembly and post-irradiation examination (PIE) of the samples. Planned measurements include inspection and electrical tests of the failed coaxial cables and electrical conductivity as a function of test temperature for the irradiated specimens. Optical absorption, fluorescence and scattering, thermal conductivity, and transmission electron microscopy examination of the specimens may also be performed.

REFERENCES

- 1 S.J. Zinkle and E.R. Hodgson, *J. Nucl. Mater.* 191-194 (1992) 58.
- 2 L.W. Hobbs, F.W. Clinard, Jr., S.J. Zinkle and R.C. Ewing, *J. Nucl. Mater.* 216 (1994) 291.

In-core ohmic check on Crystal Systems
"Hemex" UV-grade sapphire, c-axis (reactor off)



Ohmic check on sapphire during HFIR irradiation
(Crystal Systems "Hemex" UV grade, c-axis)

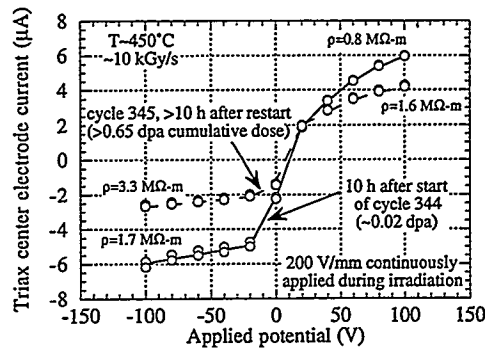


Fig. 6. Comparison of the electrical behavior of UV grade sapphire (sample 2) at 10 Gy/s and 10 kGy/s at the start of the first and second irradiation cycles.

3. S.J. Zinkle and C. Kinoshita, in Fusion Materials Semiannual Progress Report for the Period Ending Dec. 31, 1995, DOE/ER-0313/19, p. 229; also C. Kinoshita and S.J. Zinkle, proc. 7th Int. Conf. on Fusion Reactor Materials, Obninsk, Russia, J. Nucl. Mater. (in press).
4. E.R. Hodgson, Cryst. Latt. Def. Amorph. Mater. 18 (1989) 169.
5. A. Möslang, E. Daum and R. Lindau, proc. 18th Symp. of Fusion Technology, Karlsruhe, Germany, August 1994, p. 1313.
6. E.R. Hodgson, J. Nucl. Mater. 212-215 (1994) 1123.
7. W.S. Eatherly et al., in Fusion Materials Semiannual Progress Report for the Period Ending Dec. 31, 1995, DOE/ER-0313/19, p. 241.
8. A.L. Qualls, W.S. Eatherly, D.W. Heatherly, M.T. Hurst, D.G. Raby, R.G. Sitterson, L.L. Snead, K.R. Thoms, R.L. Wallace, and S.J. Zinkle, in Fusion Materials Semiann. Prog. Report for the period ending June 30, 1996, DOE/ER-0313/20, this report.
9. S.J. Zinkle, G.P. Pells and F.W. Clinard, Jr., in Fusion Reactor Materials Semiannual Progress Report for the Period Ending Sept. 30, 1993, DOE/ER-0313/15, p. 417.
10. D.P. White, in Fusion Materials Semiannual Progress Report for the Period Ending Sept. 30, 1994, DOE/ER-0313/17, p. 346.
11. E.H. Farnum, T. Shikama, M. Narui, T. Sagawa and K. Scarborough, J. Nucl. Mater. 228 (1996) 117.
12. L.L. Snead, D.P. White and S.J. Zinkle, in Fusion Materials Semiannual Progress Report for the Period Ending March 31, 1995, DOE/ER-0313/18, pp. 385-396; also J. Nucl. Mater. 226 (1995) 58.
13. L.L. Snead, D.P. White, W.S. Eatherly and S.J. Zinkle, in Fusion Materials Semiannual Progress Report for the Period Ending Dec. 31, 1995, DOE/ER-0313/19, p. 249.
14. J.J. O'Dwyer, The Theory of Dielectric Breakdown of Solids (Oxford Univ. Press, London, 1964).